# HOKKAIDO UNIVERSITY

| | |
|---|---|
| Title | Chemical Compositions and Paragenesis of the Platinum-group Element Minerals in the Jinchuan Sulfide Deposit, Gansu Province, China |
| Author(s) | Yang, Xuan-Zhu; Matsueda, Hiroharu; Yui, Shunzo; Dong, Xian-Yang |
| Citation | , 23(2), 287-299 |
| Issue Date | 1992-08 |
| Doc URL | http://hdl.handle.net/2115/36784 |
| Type | bulletin (article) |
| File Information | 23-2_p287-299.pdf |

Instructions for use

# CHEMICAL COMPOSITIONS AND PARAGENESIS OF THE PLATINUM-GROUP ELEMENT MINERALS IN THE JINCHUAN SULFIDE DEPOSIT, GANSU PROVINCE, CHINA

*by*

**Xuan-Zhu Yang, Hiroharu Matsueda,
Shunzo Yui and Xian-Yang Dong***

(with 3 text-figures, 4 tables)

*Abstract*

A variety of platinum group minerals (PGM) occurs in the Jinchuan deposit, China. Four different PGM assemblages have been distinguished as follows: The first group, mainly sperrylite, occurs within altered olivines. The second occurs within sulfide mineral grains and is composed of platinum- and palladium-dominated tellurides, bismuth tellurides. The third occurs at the margin of sulfide minerals, and includes platinum- and palladium-dominated bismuth tellurides, tellurobismuthides and sperrylites. The fourth group is composed of platinum- and palladium-dominated tellurobismuthides and bismuthides, and occurs in the fractures of sulfide minerals.

Their chemistry and mineral paragenesis indicate different origins for the four PGM groups. The first and fourth PGM groups clearly display secondary alteration products as a result of serpentinization of the host rocks. The second group represents primitive PGM formed during the sulfide crystallization stage. The third group could have been formed during the last crystallization stage of the sulfide melt. Based on these facts, a model for the remobilization and deposition of PGE is proposed for this deposit.

## Introduction

The Jinchuan deposit of China, located at the margin of the Sinokorea Precambrian shield, was discovered in 1958. The study of the platinum group elements (PGE) and platinum group minerals (PGM) from Jinchuan deposit began in 1962. But little informations were published by S. G. T. (1984) in spite of considerable attention being focussed on PGE deposit and PGM during the past 30 years. Recently, the sulfides and PGM of the deposit have been the subject of several papers (Sun, 1986; Yang, 1989; Yang *et al.*, 1991; Tang, 1991; Jia, 1986).

The purpose of this paper is to clarify chemical composition and to classify paragenesis of the various PGM associated with sulfides and silicates in this deposit. This information suggests that the PGE and Cu-Ni deposit and related ultrabasic rocks are not static after their formation as a result of magmatic processes. The presence of volatile-rich (particularly Cl-rich) fluids and alteration can play a significant role in the formation of PGE deposit (Yang, 1989).

In addition to the detailed mineralogy of PGM, minor osmium and platinum contents in hessite are also described.

## Outline of geology and ore deposits

A.  Geology

The geology of the Jinchuan ore deposits was described in detail by S. G. T. (1984), Jia (1986), Yang (1989), Yang *et al.*, (1991) and Tang (1991). The most recent information reported that the Jinchuan complex intruded into late Archean metasedimentary rocks consisting of various gneisses, chlorite-guartz schists, banded marbles and migmatite (Tang, 1991).

The Jinchuan complex is considered to be a layered ultrabasic intrusion. The principal mineral assemblage of this intrusion is olivine + orthopyroxene + clinopyroxene + plagioclase. Olivine and orthyopyroxene are commonly dominant minerals, occurreing at the bottom of the intrusion. The volume of metal sulfide minerals generally increases towards the base of the complex.

The intrusion is made up of rocks containing various proportions of cumulative olivine, bronzite, endiopside, augite and labradorite (S. G. T., 1984; Yang *et al.*, 1991). The sulfide concentration changes with different intrusion stages, generally increasing from early to later stages (Yang *et al.*, 1992).

B.  Ore deposits

The doposits consist of hundreds of orebodies. Most of them occur in the middle and bottom parts of the intrusion. Five main types of sulfide texture are observed in the deposit; (a) sideronitic texture: sulfide minerals are present as nets among the grains of olivine and pyroxene and occur as irregular blobs ranging from 1 mm to several mm; (b) disseminated texture: the sulfide minerals are located in part of the interstitial voids among silicate minerals; (c) massive texture: almost all the mineral consists of sulfide minerals; (d) veinlet texture: sulfide minerals occur in the fractures of sulfide and silicate minerals; (e) cataclastic texture: the sulfide minerals were broken into pieces, microspinifex, microreticulated, microfolded and mylonitic. The microspinifex texture is a special fecture which exhibits herringbone intergrowths of altered silicate, sulfide and magnetite, representing the pseudomorphic replacement of pentlandite. The disseminated sulfide orebodies usually occurred in the upper part, forming " hanging horizons". The sideronitic orebodies occur at the bottom part of the intrusion. The massive sulfide orebodies were formed along the contacts between different stage intrusion and occur as wide vein. The fine veinlets are distributed in all of the orebodies mentioned above. The cataclastic ores is generally rich in PGE.

The disseminated and sideronitic sulfides consist of two types: one is generated during the magmatic stage, and the other is a post-crystallization product that has been modified during alteration and now occurs as a disseminated and sideronitic ore distributed in altered silicates minerals. Although in both, the base mineral

assemblage is chalcopyrite, pyrrhotite and pentlandite; the latter contains cubanite, mackinawitie and magnetite more than the former. The latest mineralization is represented by veinlets and stringers of redistributed sulfides which traverse all oxide, silicate, and older sulfide minerals.

The ore mineral assemblages associated with PGM may be classified as follows: (1) pyrrhotite + pentlandite + chalcopyrite, (2) mackinawite + pyrrhotite + valleriite + pentlandite + chalcopyrite, and (3) chalcopyrite + cubanite + magnetite + pentlandite + mackinawite.

Assemblage 1 represents the original major primary minerals. Assemblage 2 in which chalcopyrite and pentlandite are the most abundant, usually contains a variety of other minerals as inclusions, and have been altered. Assemblage 3 comprises about 60% of PGM. Pentlandite and chalcopyrite in the assemblage exhibit complicated intergrowth and have been replaced by valleriite and mackinawite, respectively.

### Analytical procedures

Approximately 100 polished sections were systematically and carefully examined under the microscope for base metal sulfides, oxides and PGM. Electron microprobe analyses were carried out at Xi'an lnstitute of Geology and Minerals Resources, China as well as the Department of Geology and Mineralogy, Faculty of Science, Hokkaido University, Japan. Analyses of all PGM and PGE-bearing minerals were carried out by wavelength dispersion spectrometry. Operating conditions comprised an accelerating voltage of 20 kv, specimen current of 20 nA, a 20 sec count time on samples and standards, and a beam diameter of about 2 um. The following X-ray and standard materials were used: synthetic PbS for Pb M$\alpha$ and S K$\alpha$; gold-silver alloy for Au L$\alpha$ and Ag L$\alpha$; metallic GaAs for As L$\alpha$; metallic Pt, Pd, Rh, Os, Te, Bi, Cu, Ni for Pt L$\alpha$, Pd L$\alpha$, Rh L$\alpha$, Os L$\alpha$, Te L$\alpha$, Bi L$\alpha$, Cu K$\alpha$ and Ni K$\alpha$, respectively. Data were reduced using a computer program prepared by JEOL (Hirata, 1985). The program includes atomic number corrections by Philiber and Tixier (1968), absorption correction by Philibert (1963) and characteristic fluorescence corrections by Reed (1965). Owing to the smaller size of the PGM than the primary and secondary excitation area in electron microprobe analysis, apparent concentrations of some elements such as Fe, Cu, S, etc. in some PGM may be attributed in part to radiation generated in the nearby base metal sulfides,

### Mineralogy of PGM and related minerals

More than 20 PGM species and their varieties have been identified in the Jinchuan deposits (S. G. T., 1984). Approximately half of the PGM identified in amount are sperrylites and Pd-Bi-Te minerals which seem to be significant platinum and palladium carriers. The remaining PGE usually occur as metallic admix-

ture and rarely form indepentent mineral phases.

In various ore types, PGE mineralization is associated with sulfide Ni-Cu ore, especially with Cu-rich ore. PGM are common in sideronitic, veinlets and disseminated ores which have undergone romobilization. The amount of PGM markedly increases, with an increase in copper content in the ores.

PGE mineral distribution in the Ni-Cu ores are affected by alteration with various degree which has generally resulted in the redistribution of the PGE.

The spatial distribution of PGM was studied by collecting about 100 samples comprising all the rock and ore types from the drill cores and open pits. They are classified into four groups as follows: (A) Arsenides, (B) Tellurides, (C) Bismuthides, (D) Tellurobismuthides, (E) Osmium-bearing minerals.

A.  Arsenides

The PGE-arsenides found in the samples of the Jinchuan deposit occur mainly as sperrylite ($PtAs_2$) which is the most common mineral and constitutes about 30%

Table 1  Electron microprobe analyses of sperrylites from the Jinchuan Deposits.

| No. | 1 | 2 | 3 | 4 | 5 |
|---|---|---|---|---|---|
| Types | I | II | II | III | IV |
| Wt. % | | | | | |
| Pt | 57.01 | 56.44 | 54.81 | 53.93 | 56.06 |
| Pd | | 0.00 | 0.15 | 0.00 | 0.00 |
| Rh | | 0.25 | 0.10 | 0.00 | 0.00 |
| Fe | | 0.04 | 0.24 | 0.14 | 0.51 |
| Ni | | 0.00 | 0.00 | 0.09 | 0.04 |
| Cu | | 0.03 | 0.01 | 0.85 | 0.33 |
| Pb | | 0.00 | 0.00 | 0.00 | 0.00 |
| As | 43.13 | 43.03 | 44.85 | 42.68 | 44.08 |
| Te | | 0.00 | 0.00 | 0.00 | 0.00 |
| S | | 0.03 | 0.19 | 1.08 | 0.20 |
| Total | 100.14 | 99.82 | 100.35 | 98.77 | 101.22 |
| Atom. % | | | | | |
| Pt | 33.67 | 33.32 | 31.49 | 30.81 | 32.04 |
| Pd | | 0.00 | 0.16 | 0.00 | 0.00 |
| Rh | | 0.28 | 0.11 | 0.00 | 0.00 |
| Fe | | 0.08 | 0.48 | 0.28 | 1.02 |
| Ni | | 0.00 | 0.00 | 0.17 | 0.08 |
| Cu | | 0.05 | 0.02 | 1.49 | 0.58 |
| Pb | | 0.00 | 0.00 | 0.00 | 0.00 |
| As | 66.33 | 66.15 | 67.08 | 63.49 | 65.59 |
| Te | | 0.00 | 0.00 | 0.00 | 0.00 |
| S | | 0.11 | 0.66 | 3.75 | 0.70 |

of all PGM.   Almost all sperrylites are range from 2-50 $\mu$m, and some are 100 $\mu$m in size.   Sperrylites examined can be devided into four types in modes of occurrence.   The first is as crystal bridges occurring between sulfides (Table 1, I, Text-
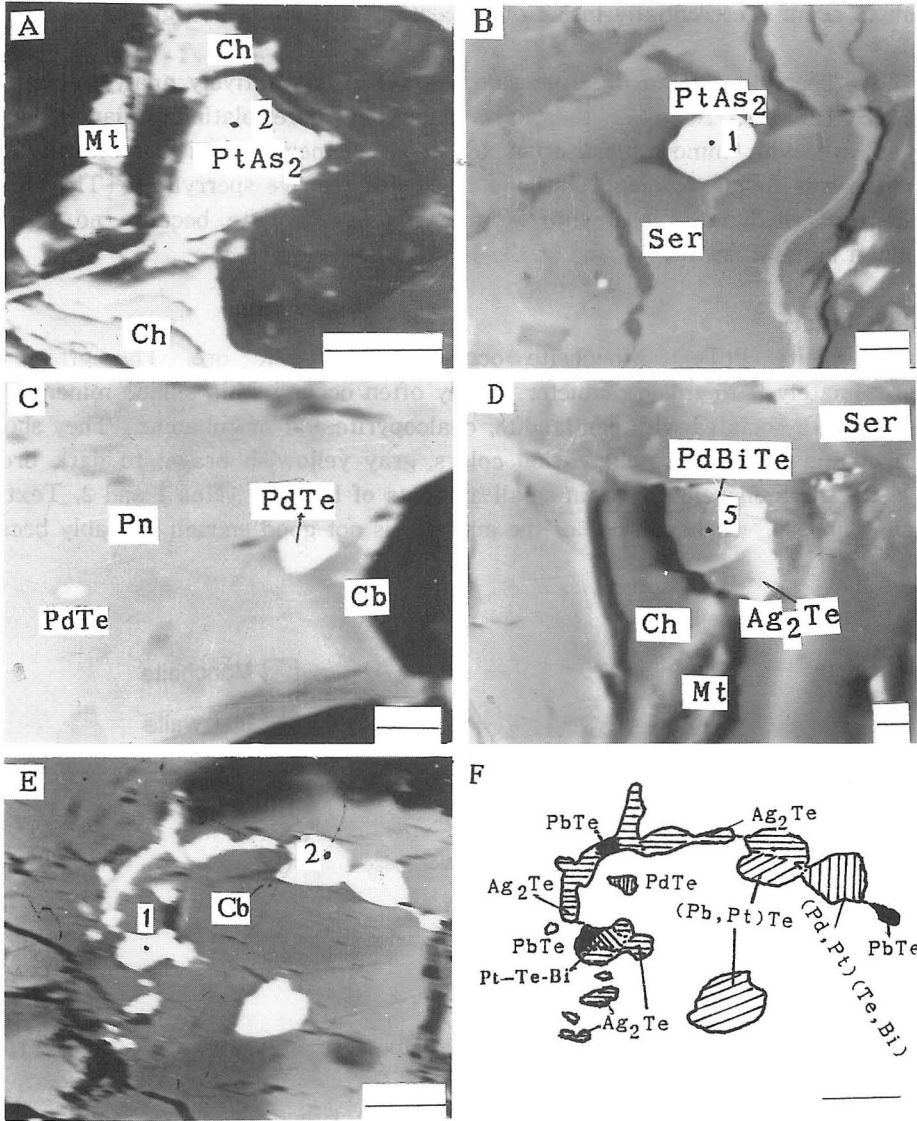


**Text-fig. 1** Back-scattered electron images (A, B, C, D and E) of PGM and sketch map (F). A and B: different occurrence of sperrylites (PtAs$_2$);  C: merenskyite (PdTe$_2$) occured in the pentlandite;  D: michenerite (PdBiTe) and hessite (Ag$_2$Te) occurred in margin of the chalcopyrite;  E and F: PGM occurred in sulfide and its sketch map.   Scale bar : 10 $\mu$m.
Abbreviations : Cb=Cubanite;   Mt=Magnetite;   Pn=Pentlandite; Ch=Chalcopyrite;   Ser= Serpentine.   See Table 1 for Nos. 1 in B & 2 in A;   Tables 2 & 4 for Nos. 1 & 2 in E, respectively;   Table 3 for 5 in D.

fig. 1A) ; the second is as large euhedral crystals occurring in altered silicates and/ or in the fractures of serpentine (Table 1, II, Text-fig. 1B) ; the third is as euhedral occurring between sulfide and altered silicate minerals (Table 1, III) ; and the fourth is as small grains occurring in sulfide minerals (Table 1, IV). Larger grains seem to occur preferentially inside of serpentines and at the margin of sulfide minerals.

Five sperrylites from different samples were quantitatively analyzed with the EPMA (Table 1). Some of them are essentially pure platinum diarsenide and others are with minor substitution by some elements. It is noteworthy that rhodium was found replacing platinum in two of the five sperrylites. The various content of rhodium in sperrylite is important as to date, because no separate rhodium mineral has been found at the Jinchuan deposits.

B. Tellurides

Moncheite (PtTe$_2$) : Moncheite occus in sideronitic ore. The grains are approximately 5-25 $\mu$m in diameter. They often occur within sulfide minerals and are closely associated with pentlandite, chalcopyrite and/or cubanite. They show a distinct and strong the polarization colors, gray yellowish brown to dark brown. Some of the moncheites contain small amounts of bismuth (Nos 1 and 2, Text-fig. 2 and Table 2). Although one of the analyses is not good enough probably because
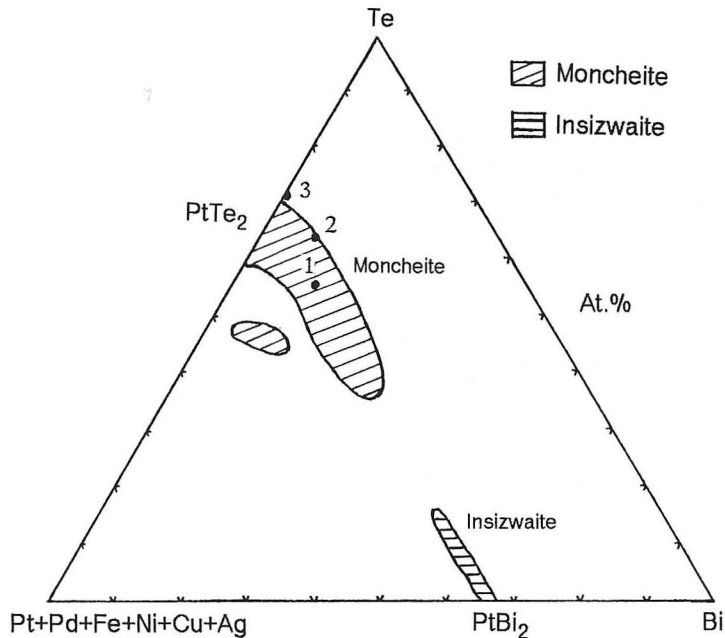


**Text-fig. 2**  (Pt+Pd+Ag+Fe+Ni+Cu)-Bi-Te diagram showing the compositional variation of moncheites from the Jinchuan deposit (No. 1 to 3 are shown in Table 2). Shaded areas represent the compositional fields of different PGM (D. M. W. Harney and R. K. W. Merkle, 1990).

of its small grain size, it seems to be moncheite.

Merenskyite (PdTe$_2$): Merenskyite occurs in sideronitic and disseminated ore as grains ranging between 4-20 $\mu$m in diameter. They are intergrown with chalcopyrite and/or pentlandite (Text-fig. 1C). The chemical composition by EPMA is given in Table 3 (No. 1) and shown in Text-fig. 3. It is actually bismuthian merenskyite.

Kotulskite (PdTe): Kotulskite occurs as anhedral grains with a diameter between 5-18 $\mu$m. It also usually occurs

**Table 2** Electron microprobe analyses of moncheites from the Jinchuan Deposits.

| No. | 1 | 2 | 3 |
|---|---|---|---|
| Wt. % | | | |
| Pt | 41.60 | 37.80 | 37.50 |
| Te | 41.49 | 44.50 | 62.60 |
| Bi | 16.80 | 14.80 | |
| Total | 99.89 | 97.10 | 100.10 |
| Atom. % | | | |
| Pt | 34.46 | 31.59 | 28.15 |
| Te | 52.55 | 56.86 | 71.85 |
| Bi | 12.99 | 11.55 | |

as grains at the margin of chalcopyrite and magnetite or cubanite. The chemical composition of kotulskite (Table 3, No. 2) indicates the minerals are bismuthian

**Table 3** Electron microprobe analyses of merenskyite (No. 1), Kotulskite (No. 2), Minchenerites (Nos. 3 & 5) and froodites (Nos. 6 & 7) from the Jinchuan Deposits.

| No. | 1 | 2 | 3 | 4 | 5 | 6 | 7 |
|---|---|---|---|---|---|---|---|
| Wt. % | | | | | | | |
| Pt | 0.00 | 0.00 | 0.28 | 0.15 | 0.34 | 7.30 | 1.20 |
| Pd | 19.90 | 15.85 | 20.90 | 20.40 | 17.74 | 16.60 | 15.80 |
| Ag | 0.35 | 8.80 | 8.30 | 0.00 | 0.57 | 0.40 | 4.70 |
| Fe | 1.21 | 1.78 | 1.15 | 1.30 | 3.81 | 0.00 | 0.00 |
| Co | 0.00 | 0.45 | 0.00 | 0.00 | 0.48 | 0.00 | 0.00 |
| Ni | 4.80 | 1.84 | 0.00 | 2.35 | 0.00 | 0.00 | 0.00 |
| Cu | 0.34 | 1.62 | 0.00 | 0.00 | 3.64 | 0.00 | 0.00 |
| As | 0.00 | 0.82 | 0.27 | 0.00 | 0.00 | 0.00 | 0.00 |
| Te | 42.80 | 25.02 | 26.80 | 38.00 | 24.07 | 0.00 | 0.34 |
| Bi | 26.80 | 40.09 | 43.80 | 38.80 | 47.43 | 76.80 | 77.93 |
| S | 2.30 | 1.75 | 0.00 | 0.30 | 1.81 | 0.00 | 0.00 |
| Total | 98.50 | 98.02 | 101.50 | 101.30 | 99.89 | 101.10 | 99.97 |
| Atom. % | | | | | | | |
| Pt | 0.00 | 0.00 | 0.20 | 0.10 | 0.22 | 6.63 | 1.07 |
| Pd | 22.41 | 19.09 | 27.33 | 25.61 | 21.39 | 27.63 | 25.88 |
| Ag | 0.39 | 10.45 | 10.71 | 0.00 | 0.68 | 0.66 | 7.59 |
| Fe | 2.60 | 4.08 | 2.87 | 3.11 | 8.75 | 0.00 | 0.00 |
| Co | 0.00 | 0.98 | 0.00 | 0.00 | 1.04 | 0.00 | 0.00 |
| Ni | 9.80 | 4.02 | 0.00 | 5.35 | 0.00 | 0.00 | 0.00 |
| Cu | 0.64 | 3.27 | 0.00 | 0.00 | 7.35 | 0.00 | 0.00 |
| As | 0.00 | 1.40 | 0.50 | 0.00 | 0.00 | 0.00 | 0.00 |
| Bi | 15.37 | 24.58 | 29.17 | 24.80 | 29.12 | 65.09 | 64.99 |
| Te | 40.20 | 25.13 | 29.23 | 39.78 | 24.20 | 0.00 | 0.46 |
| S | 8.60 | 6.99 | 0.00 | 1.25 | 7.24 | 0.00 | 0.00 |

X. Z. Yang et al.
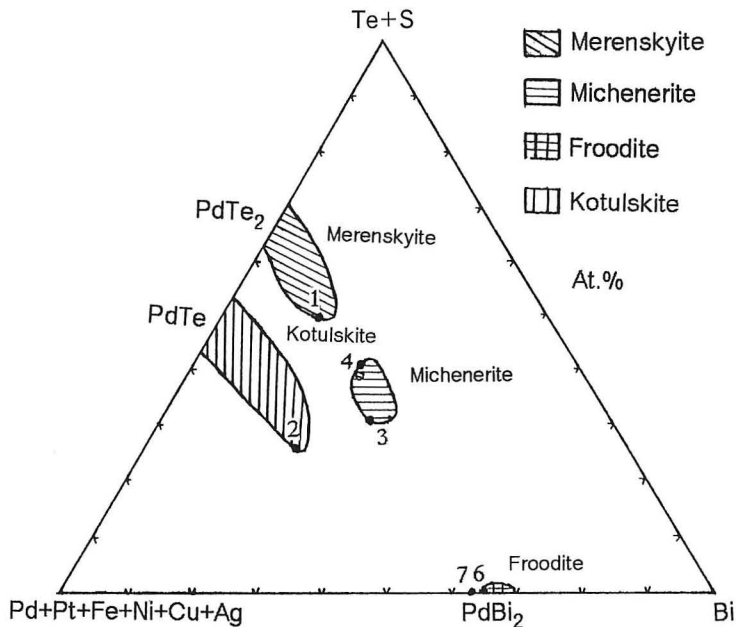


**Text-fig. 3** Compositions of natural Pt-Pd-Bi-Te minerals from the Jinchuan deposit (Nos. 1 to 4, 6 and 7 are shown in Table 3) in the (Pt+Pd+Ag+Fe+Ni+Cu)-Bi-(Te+S) diagram. Shaded areas represent the compositional fields of different PGM (D. M. W. Harney and R. K. W. Merkle, 1990).

kotulskite containing 8.8% Ag.

Hessite ($Ag_2Te$): Hessite generally occurs as fine-grained (5-20 $\mu$m) crystals at the margin of palladium minerals and altered olivine, or at the margins of the chalcopyrite (Text-fig. 1D). Coarse hessite which occurs in mineral fractures co-exists with cubanite and is usually intergrown with altaite and palladium minerals (Text-fig. 1E and F). It also penetrates into the contact between sulfide and silicate mineral. The compositions of the hessites are shown in Table 4 and the grains are mainly composed of silver and tellurium with small amount of Se, Cu, etc. Although the analyses are not good enough probably because of their small grain size, they seem to be hessite.

Altaite (PbTe): Altaite has been discovered in disseminated, sideronitic, massive, vein and metasomatic ores. It occurs as discrete crystals (5-30 $\mu$m) in chalcopyrite and/or cubanite (Text-fig. 1E and F), and single crystal in pentlandite. The sketch map (Text-fig. 1F) is based on the characteristic X-ray images which indicate some of altaites are impure PbTe with small amount of Pt. It may be significant that minor platinum is stored in altaite and may be a new source of platinum.

C. Tellurobismuthide

Michenerite (PdBiTe): Michenerite occurs as rounded or subhedral crystals in

some chalcopyrite, cubanite and pentlan-
dite and at the border with hydrous sili-
cate minerals of disseminated and sider-
onitic ores (Table 3 and Text-fig. 1D, No.
5). Most grains are 5-25 $\mu$m in diameter.
It is usually isotropic and some show
anisotropism with a brown to greenish-
gray tinge. The latter (Table 3, No. 4)
are slightly lower in bismuth content than
the former (Table 3, Nos. 3 and 5). The
compositional change is exhibited in
Text-fig. 3. Silver, platinum may, in
part, substitutes for palladium. One
analysis (No. 5 of Tabe 3) contains con-
siderable amount of Cu, Fe, S etc. They
may be attributed to neighbouring base
metal monosulfides, therefore, the true
values for the mineral are recalculable by
deleting sulfur and corresponding metals.

### D.  Bismuthide

Froodite (PdBi$_2$) : Froodite occurs
along fractures and at the margins of the
chalcopyrite, magnetite and pentlandite in
disseminated ores. It varies in diameter
from less than 5 $\mu$m to 30 $\mu$m, and is usu-
ally anhedral, sometimes oval in shape.
The chemical composition is shown in
Table 3 and Text-fig.3 (No. 6 to 7). It
contains platinum and silver as (Pd, Pt,
Ag) Bi$_2$, but does not contain so much
tellurium as in other PGE deposits (Vol-
borth, *et al.*, 1986).

**Table 4** Electron microprobe analyses of hessites from the Jinchuan Deposits.

| No. | 1 | 2 |
|---|---|---|
| Wt. % | | |
| Pt | 0.28 | 0.12 |
| Pd | 0.13 | 0.00 |
| Os | 1.97 | 0.00 |
| Ag | 49.77 | 52.74 |
| Fe | 0.00 | 5.02 |
| Co | 0.12 | 0.00 |
| Ni | 0.12 | 0.00 |
| Cu | 2.31 | 2.10 |
| Pb | 0.00 | 7.18 |
| As | 0.14 | 0.39 |
| Te | 37.04 | 29.85 |
| Bi | 0.83 | 0.00 |
| Se | 3.90 | 0.00 |
| Total | 96.61 | 97.40 |
| Atom. % | | |
| Pt | 0.17 | 0.07 |
| Pd | 0.14 | 0.00 |
| Os | 1.20 | 0.00 |
| Ag | 53.63 | 55.17 |
| Fe | 0.00 | 10.14 |
| Co | 0.24 | 0.00 |
| Ni | 0.24 | 0.00 |
| Cu | 4.23 | 3.73 |
| Pb | 0.00 | 3.91 |
| As | 0.22 | 0.59 |
| Te | 33.74 | 26.40 |
| Bi | 0.46 | 0.00 |
| Se | 5.74 | 0.00 |

### E.  Rhodium and osmium-bearing minerals

No rhodium and osmium minerals were found in the samples from the Jinchuan
deposit. It is considered that rhodium and osmium elements were in the base metal
sulfides, particularly pentlandites, either as a solid solution or as submicrostpic
inclusions (S. G. T., 1984). However, one osmium-rich minerals were found at the
deposit during this study. The analysis gave a composition of 1.97 wt% Os in
hessite (Table 4, No. 1). Sperrylite in the occurrence of type II contains some
rhodium (Table 1, Nos. 1 and 2).

## Paragenesis of the PGM

Based on the descriptions above, PGM paragenesis in the Jinchuan deposit can be divided into four categories: (a) PGM in serpentines (Text-fig. 1B), (b) PGM in sulfide minerals (Text-fig. 1C), (c) PGM occurring in sulfide minerals bordering on altered silicate minerals (Text-fig. 1D), and (d) PGM occurring along the fractures of sulfide minerals (Text-fig. 1E).

Paragenesis (a): the major PGM is sperrylite, sometimes intergrown with other PGM and sulfide minerals.

Paragenesis (b): PGM are mainly PGE tellurides. They are smaller in size and characterized by moncheites, hessite, altaite, kotulskite and merenskyite paragenesis. The bismuth content in these minerals is lower than that of the PGM of paragenesis (c) and (d). Associated sulfides are chalcopyrite, pentlandite and pyrrhotite which generally represent primary mineral paragegesis of the earlier stage of mineralization.

Paragenesis (c): PGM are commonly coarse-grained PGE bismuth tellurides and tellurides as well as sperrylites. PGM paragenesis is dominated by bismuth moncheites, michenerite, bismuth kotulskite, bismuth merenskyite and hessite. Associated sulfides are mainly chalcopyrite, pentlandite with cubanite showing primary minerals characterized by weak alteration.

Paragenesis (d): PGM are dominantly PGE tellurium bismuthides and bismuthides. PGM association are characterized by platinum altaite, michenerite, and froodite and hessite. Associated minerals are cubanite, chalcopyrite, mackinawite and magnetites which are usually replaced and remobilized.

The microscopic and compositional investigations above indicate that the PGM (particularly, telluride and bismuthide) usually occur with hessite and altaite. This suggests their contemporaneous crystalization. The elemental substitution also indicates a close relationship between bismuth and tellurium with palladium and silver (Yang, 1989). Platinum- and palladium-bearing sulfide minerals have not been discovered.

## Discussion

The presence of PGM within sulfide minerals and at the margin of sulfide minerals, indicates that the PGM were extracted from the sulfide melt. PGM, present in altered silicate minerals and the fractures of sulfide minerals, illustrate that the PGE underwent remobilization by postmagmatic fluids.

A. The role of sulfide liquids and volatiles

The close relationship between platinum and palladium with nickel and copper clearly demonstrates that the sulfide liquid acted as a collector of PGE derived from the silicate magma. The PGE partition into sulfide melt has also been proven by Campbell and Barnes (1984) and Naldrett and Barnes (1986). However, a lot

of sperrylites occur in serpentine and in fractures of magnetite without direct contact with base metal sulfide minerals. It is difficult to explain this textural peculiarity on the assumption of a magmatic concentration process in which PGE were trapped by the sulfide melt. Yang (1989) suggested that the occurrence of sperrylite may be attributed to the role of volatile based on the inclusion studies.

Many features suggested that these PGM crystallized at a relatively late stage. In particular, PGM are concentrated in altered and fractured zones of the intrusion and have not been observed in the unaltered silicate minerals of the studied samples. During serpentinization, the PGE are liberated and extracted from sulfide minerals, and enriched into fluids and then they are redeposited as independent minerals. Part of them crystallized in serpentinized olivines, some close to the sulfide minerals. The highest concentration of platinum in the altered rocks suggests that the redeposition of platinum took place during the post-magmatic stage or at a much late stage (S. G. T., 1984). The positive correlation between the degree of serpentinization and the abundance of PGE reported by Yang (1989) supports this idea. The high Cl content of the serpentine (0.40 wt%) and apatite (1.73 wt%) in contact with the sulfides and PGM further suggests that chloride complex played a significant role in the transportation and deposition of the PGM during the hydrothermal event (Yang et al., 1992, in press).

The results of the mineralogical study indicate that the behavior of palladium differs slightly from that of platinum, as has been proven by the PGM paragenesis in this study. Most palladium may be enriched in sulfide phases, especially in the Cu-rich residual melt, where it crystallized as tellurides and bismuthides together with silver minerals (Text-fig. 1D). We appreciate Ballhaus and Stumpfl's (1986) idea. They stated that most precious elements form chloride complex, and PGM were formed by breakup of the complex bond.

Taking these factors into account, we consider that most of the PGE are enriched in volatiles and sulfide melt. During crystallization of the sulfied melt, some PGE first crystallize as PGM, but others are progressively concentrated into volatiles and the remaining sulfide melt (Cu-rich). Finally, the volatiles not only alter earlier minerals, but also expell PGE from them to the sulfide periphery and the fractures of the sulfide and magnetite minerals, and then crystallize as PGM.

B. Crystallization temperature of PGM

Determination of the crystallization temperature of the PGM is difficult because there is no direct method of measurement, but it can be estimated by experimental data. Hoffman and MacLean (1976) found that formation temperatures of pure kotulskite and merenskyite were 720℃ and 740℃, respectively, on the basis of the Pd-Te-Bi ternary system. Actual crystallization temperatures may be lower because of the presence of additional elements in the system during PGM crystallation. While the stability field of both merenskyite and michenerite is estimated above 450℃ and below about 490℃, Hoffman and MacLean (1976) found that the melting temperature of michenerite strongly depends on the tellurium and bismuth

concentrations and varies from 489 (Bi-rich) to 501℃ (Te-rich). Therefore, intergrowth between merenskyite and kotulskite may be used as a geothermometer. According to the actual PGM association and their chemical compositions in the Jinchuan deposit, it is estimated that the upper limit of the temperature of crystallization of PGE bismuth-tellurides are about 720℃, indicating PGM association (b) enclosed in sulfide minerals; while the lower temperature limit is about 450℃, PGM association (c) and (d) occurring at the margin and in the fractures of the sulfide minerals. Therefore, formation temperature of PGM could be in the range of 450-720℃ in the Jinchuan deposit. The result of this study shows that the temperatures of crystallization of PGM gradually reduce according to their mode of paragenesis from (b), (c) to (d). This is consistent with the experiments of Hoffman and MacLean (1976). Sperrylite found in serpentine seems to crystallize from hydorothermal fluid below about 450℃, the approximate temperature of serpentinization of olivine.

## Conclusion

It has been demonstrated that the dominant PGM are palladium and platinum minerals, but iridium, osmium, ruthenium and rhodium minerals are absent in the Jinchuan deposit. PGM paragenesis can be divided into 4 categories mentioned above. It is interesting to note that some precious minerals tend to occur at the BMS-gangue contacts (paragenesis c). This may suggest the role of volatiles. A part of the PGE remain in the Fe-Ni monosulfide and crystallized as PGM which are now associated with pyrrhotite and pentlandite (paragenesis b). A lot of precious metal minerals occur in the altered silicate minerals and fractures of sulfide minerals (paragenesis a and b). This may be related to post-magmatic hydrothermal alteration event but not directly linked to the magmatic crystallization. Magmatic inclusion and fluid inclusion as well as secondary fluid inclusion data from the Jinchuan deposit have provided support for this hypothesis (Yang *et al*, 1991).

The major formation temperature of PGM at Jinchuan deposit are in range of 450-720℃

It is also an important discovery that rhodium, and platinum and osmium, occur in sperrylite, and altaite and hessite, respectively. This may provide a new resource for those elements.

*References*

Ballaus, C. G. and Stumplf, E. F, 1986. Sulfide and Platinum mineralization in the Merensky Reef : evidence from hydrous silicates and fluid inclusions. *Contrb. Mineral. Petrol.*, 94 : 193-204.

Barnes, S. J. and Campbell, I. H., 1988. Role of late magmatic fluids in Merensky-type platinum deposits : A discussion. *Geology*, 16 : 488-491.

Cabri, L. J. and Laflamme, J. H. G., 1976. The mineralogy of the platinum-group elements from copper-nickel deposits of the Sudbury Area, Ontario. *Econ. Geol.*, 71 : 1159-1195.

Campbell, I. H. and Barnes, S. J., 1984. A model for the geochemistry of the platinum-group elements in magmatic sulfide deposit. *Can. Mineral.*, 22 : 151-160.

Harney, D. M. W. and Merkle, R. K. W., 1990. Pt-Pd minerals from the upper zone of the eastern Bushveld complex, South Africa. *Can. Mineral.*, 28 : 619-628.

Hirata, 1985. Quantitative Microanalysis. In : JAPS. 141 Comittee (Editors), *Microbeam analysis*. Asakura Shoten, pp. 222-229 (in Japanese).

Hoffman, E. and MacLean, W. H., 1976. Phase relation of michenerite and merenskyite in the Pd-Bi-Te system. *Econ. Geol.*, 71 : 1461-1468.

Jia, E. H., 1986. Geological characteristics of the Jinchuan Ni-Cu sulfide deposit in Gansu province. *Mineral Deposits.*, 5 : 27-37. (in Chinese with English abstract).

McElduff, B. and Stumpfl, E. F., 1990. Platinum-Group Minerals from the Troodos Ophiolite, Cyprus. *Miner. and Petrol.*, 42 : 211-232.

Naldrett, A. J. and Barnes, S. J., 1986. The behavior of platinum-group elements during fractional crystallization and partial melting with special reference to the composition of magmatic sulfide ores. *Fortschr. mineral.*, 64 : 113-133.

Philibert, J., 1963. A method for calculating the absorption correction in electron-probe microanalysis. In : Pattee, H. H. *et al.* (Editors), *X-ray optics and microanalysis*. Academic press, New York, 379-392.

Philibert, J. and Tixer, R. 1968. Some problems with quantitative electron probe microanalysis. In : K. F. J. Heinrich (Editor), *Quantitative elelctron probe microanalysis*. NBS Special Publ. 298 : 13-33.

Reed, S. J. B., 1965. Characteristic fluorescence correction in electron-probe microanalysis. *Br. J. Appl. Phys.*, 16 : 913-926.

S. G. T. (The Sixth Geological Team of Gansu Geological Survey China), 1984. *Geology of Cu-N sulfide Deposit in Baijiazuezhi*. Geological Publication Bureau, China. 225 p. (in Chinese).

Sun, S. X., 1986. The discovery of Pt enrichment parts and existing status of Pt and Pd in mining area of Jinchuan sulfide Ni-Cu deposit. *Geology and prospecting*, 12 : 36-39. (in Chinese).

Tang, Z. L., 1991. The metallogenetic model of the Jinchuan platinum-bearing copper-nickel sulfide deposit. *International Symposium on sulfide deposit, Jinchuan, China.* 17-38.

Volborth, A. *et al.*, 1986. A survey of the Pd-Pt mineralization along the 35-km strike of the J-M Reef, Stillwater Complex, Montana. *Can. Mineral.*, 24 : 329-346.

Yang, X. Z., 1989. Platinum group and gold elements geochemisty in Jinchuan Ni-Cu sulfide deposit, Gansu Province, China. *Bull. Xi'an Inst. Geol. Min. Chinese Acad. Geol. Sci.*, 26 : 57-68. (in Chinese with English abstract).

Yang, X. Z., An, S. Y., Hou, S. J., Gong Z. C., & Dong, X. Y., 1991. The REE characteristic and petrogensis and metallogenesic significance of the Jinchuan ore-bearing ultrabasic intrusion, Gansu Province, China. *Journal of Xi'an college of geology*, 1 : 15-22. (in Chinese with English abstract).

Yang, X. Z. and Dong, X. Y., 1992. The petrogenesis and metallogenesis periods and model of the genesis in the Jinchuan ore-bearing ultrabasic intrusion, Gansu province, China. *Bull. Xi'an Inst. Geol. Min. Res., Chinese Acad, Geol. Sci.*, (in press).

Yang, X. Z., Pen, L. G., Dong, X. Y., Hou, S. J, Gong, Z. C. & An, S. Y., 1991. The magmatic inclusions characteristics and their geological sense in the Jinchuan copper-nickel bearing ultrabasic intrusion. *Geol. Review.*, 37 : 78-86. (in Chinese with English abstract).